Comparative study on structure and wetting properties of diamond-like carbon films by W and Cu doping

Lili Sun [a,b,1], Peng Guo [a,1], Xiaowei Li [a], Aiying Wang [a,*]

[a] Key Laboratory of Marine Materials and Related Technologies, Zhejiang Key Laboratory of Marine Materials and Protective Technologies, Ningbo Institute of Materials Technology and Engineering, Chinese Academy of Sciences, Ningbo 315201, PR China
[b] University of Chinese Academy of Sciences, Beijing 100049, PR China

ABSTRACT

By specifically selecting the carbide-forming metal (W) and non-carbide-forming metal (Cu) as the doped metal, we fabricated the W and Cu doped diamond-like carbon (W-DLC and Cu-DLC) films by hybrid ion beam system, respectively. And a comparative study on structure and wetting properties of W-DLC and Cu-DLC films was focused. For Cu-DLC films, the wettability transformation from hydrophilicity (76.56°) to hydrophobicity (105.6°) was observed. While in case of W-DLC films, the wettability of films maintained the hydrophilicity (73.6 ± 3.93°) within the presented W concentration. Based on the surface energy calculation and electronic structure analysis from first-principles calculations, we firstly gained insight into the wettability behavior of W-DLC and Cu-DLC films in terms of the bond characteristics formed between doped metal and C atoms. Results showed that the anti-bonding characteristic between Cu and C atoms reduced the polar components of surface energy and dangling bonds, contributing to the improvement of hydrophobic property, while the non-bonding characteristic for W—C bond resulted in the appearance of dipoles, leading to the hydrophilic character. It was in particularly concluded that the different bond characteristic between metal and C atoms played a key role in the wettability of metal doped DLC films. The obtained results offer a facile strategy to design DLC films with tailored wettability properties for the promising hydrophobic applications.

© 2016 Elsevier B.V. All rights reserved.

1. Introduction

Owing to its exceptional properties such as super-high hardness, thermal conductivity and unusual lubricity, diamond-like carbon (DLC) film has become one of the most promising engineering materials [1–2]. However, the existed high intrinsic stress and hydrophilic surface property of DLC film limit its further applications in the fields of microelectromechanical systems as stiction-reducing films [3–4]. To avoid this problem, various metal elements were usually doped into carbon matrix to adjust the properties of the film [4]. For example, introducing carbide-forming metal such as Ti into DLC films brought higher sp^2-bonded carbon and the formation of Ti—O bond, which decreased surface energy of films leading to the increase of water contact angle (WCA) from 68.5° to 105° (a material is called hydrophobic when the intrinsic WCA is >90° [5]) [6]; for non-carbide-forming metal such as Ni doped DLC film, the WCA was maintained at approximately 80°

due to the partly oxidized state of Ni [7]. However, Ostrovskaya et al. [8] reported that the doped carbide-forming metals could make the films more hydrophilic, while the non-carbide-forming metals decreased the surface energy and thus led to hydrophobicity. It is obvious that, due to the complex interaction between the doped metal and carbon atoms [9], the wettability of metal doped DLC films (Me-DLC) showed distinct dependence upon the type and concentration of the doped metal, leading to the controversy of wetting mechanism. Therefore, by combining the experiment with theoretical calculation, the further comparative and systematical understanding of the correlation between the microstructure and wetting property of Me-DLC films caused by different metals is still required.

In this work, two typical metal elements, W as carbide-forming metal with non-bonding characteristic and Cu as non-carbide-forming metal with anti-bonding characteristic [9], were selected to synthesize the Me-DLC films for comparison. The effects of surface chemical properties, structure and roughness of the films on surface energy were discussed comparatively. Moreover, the first-principles simulation was also used to clarify the mechanism of wetting properties caused by W or Cu doping from atomic scale. It could provide an effective guidance for selecting doped metals to control the wettability of DLC films for

---

promising applications such as biomedical implants and marine frictional components.

2. Experimental details

Cu doped DLC (Cu-DLC) and W doped DLC (W-DLC) films were deposited at room-temperature on crystalline silicon (P⟨100⟩) using a hybrid ion beam deposition system [10] which consisted of an anode-layer linear ion source (LIS) and a DC magnetron sputtering. Prior to the deposition, the substrates were cleaned by an ultrasonic bath using acetone and ethanol for 15 min separately. When the base pressure of chamber was about 2.7×10^{-3} Pa, the substrates were cleaned by Ar ions for 10 min. During Cu-DLC films deposition, C_2H_2 of 15 sccm was introduced into the LIS for DLC deposition; the Ar gas of 65 sccm was supplied to the magnetron sputtering, and the sputtering currents were set as 0.8, 1.0, 1.2, 1.5, 1.8 and 2.0 A to control the Cu concentration. For W-DLC films deposition, C_2H_2 of 10 sccm was introduced into the LIS for DLC deposition; the Ar gas of 70 sccm was supplied to the magnetron sputtering, and the sputtering current was changed from 1.2 to 2.0 A to adjust the W concentration. The power of LIS source was 260 W, while that of sputtering source was in range of 1300–1500 W which varied with sputtering current. For comparison, pure DLC film was also deposited.

Raman spectroscopy (inVia-reflex, Renishaw) with 532 nm excitation was employed to evaluate the carbon atomic bonds of films. The surface morphology of films in a size of 3 μm × 3 μm was observed using a Scanning Probe Microscope (Dimension 3100 V, Veeco, US), on a tapping mode, and the image analysis of the roughness (Ra) was carried out from 512 × 512 surface height data points using a Nanoscope version 7.20 software. Furthermore, the chemical composition and bonds of the films were characterized by X-ray photoelectron spectroscopy (XPS, Axis UltraDLD, Japan) with Al (mono) Kα radiation, a pass energy of 160 eV was chosen for the acquisition of surveys spectra, while a pass energy of 20 eV was chosen to enhance the energy resolution for the acquisition of high resolution spectra. High-resolution transmission electron microscope (HRTEM) was performed using a Tecnai F20 electron microscope (FEI company, Netherlands), which was operated at 200 kV with a pointed-to-point resolution of 0.24 nm. The static contact angle was measured by an OCA20 optical system (Dataphysics Ltd., Germany) in atmosphere at room temperature, 2 μl droplets of de-ionized water and diiodomethane were used as the working liquids, respectively. The measurement was operated at 5 different regions on each sample. Surface energies (SE) were calculated using water as the polar liquid and diiodomethane as the nonpolar liquid.

In order to investigate the electronic structure of W—C and Cu—C systems, the spin-polarized first-principles calculations based on the density functional theory were performed, which were implemented in the DMol^3 software package. The exchange-correlation potential was defined by the Perdew-Burke-Ernzerhof parameterization and all electrons double-numerical polarization basis set was used. Atomic bonding characteristics were analyzed by the charge distribution of the highest occupied molecular orbitals (HOMO).

3. Results and discussion

3.1. Film composition

Fig. 1 shows the W and Cu concentrations of as-deposited films as a function of sputtering current, respectively. For W-DLC films, the W concentration in the films varied from 0.3 to 34.2 at.% as the sputtering current increased from 1.2 to 2.0 A, while the Cu concentration of Cu-DLC films varied from 0.1 to 39.7 at.% with the sputtering current increasing from 0.8 to 2.0 A. This indicated that the doped metal concentration could be easily tailored through adjusting the sputtering current.
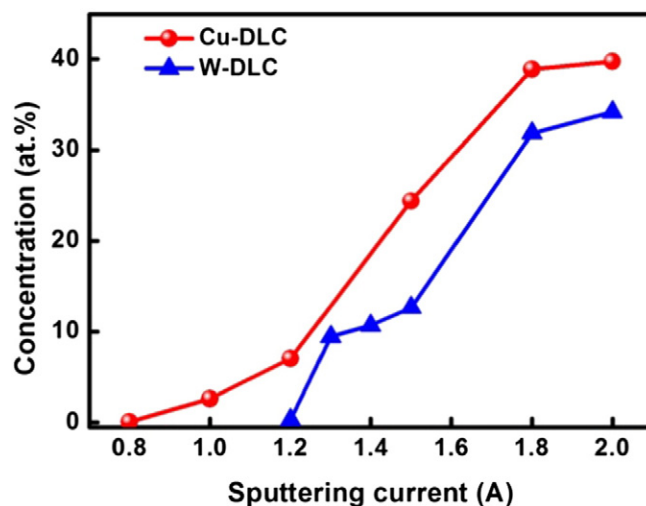

Fig. 1. W and Cu concentrations of the Me-DLC films as a function of sputtering current.

3.2. Wetting property

Fig. 2 shows the correlation between the WCA and the doped metal concentration. Pure DLC film is also evaluated for comparison. It could be seen that the contact angle of W-DLC films was approximately kept at 73.6 ± 3.93° regardless of changes in W concentrations; but for Cu-DLC films, the WCA increased dramatically (larger than 90°) when the Cu concentration was higher than 7.0 at.%. It could be deduced that, compared with pure DLC film, the DLC film was changed from hydrophilic state to hydrophobic state by the addition of Cu, while the W doping made little influence on the water wetting property of DLC films. It was revealed that the wettability of Me-DLC was strongly depended on the type and concentration of doped metals.

3.3. Microstructure

In order to explore the influence of chemical composition on wettability of W-DLC and Cu-DLC films, XPS was performed to investigate the change of surface composition [11]. Fig. 3a presents the C 1s spectra of Cu-DLC films with various Cu concentrations. The XPS C1s spectra showed a large asymmetric peak suggesting the existence of carbon atoms with various bonding states. Meanwhile, the Cu 2p spectrum of Cu-DLC film with Cu 39.7 at.% is given in Fig. 3b. There were two
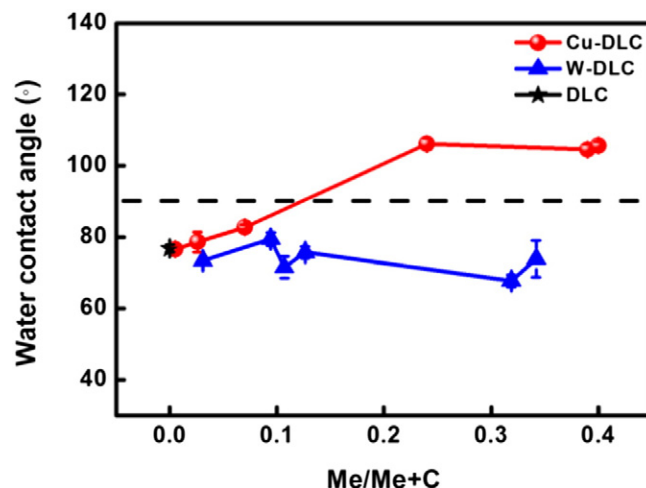

Fig. 2. Effect of W and Cu concentrations on water contact angle, and pure DLC film was also used for comparison.
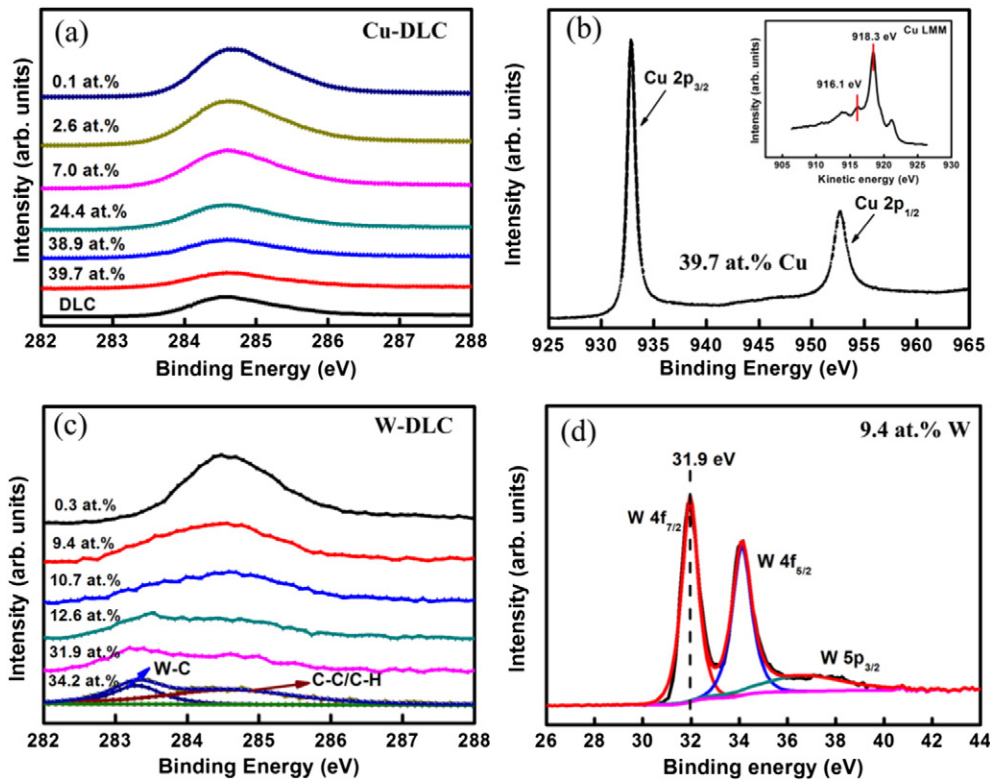
Fig. 3. XPS spectra of Cu-DLC and W-DLC films: (a) C 1s and (b) Cu 2p and Cu LMM of Cu-DLC films, (c) C 1s and (d) W 4f of W-DLC films.

peaks corresponding to Cu $2p_{1/2}$ located at 952.7 eV and Cu $2p_{3/2}$ located around 932.8 eV, due to the formation of Cu or Cu_2O (the binding energies of Cu and Cu_2O phases were very close). The Cu LMM Anger transition in XPS spectra was further carried out to distinguish Cu and Cu_2O which were located at 916 and 918 eV, respectively [12–13]. In the Cu LMM Auger spectra (inset of Fig. 3b), there were two peaks at about 916.1 and 918.3 eV, and the intensity of the peak at 918.3 eV was obviously stronger than that at 916.1 eV, suggesting the existence of Cu metal and partly Cu oxidation. It could thus be said that there was no Cu—C bonding formed in the Cu-DLC films with various Cu concentrations.

Different from Cu-DLC, Fig. 3c displays the XPS C 1s peaks of W-DLC films with different W concentrations. For the films with low W concentrations (<9.4 at.%), the C 1s spectra with a major peak around 284.5 eV was only the typical C—C/C—H binding energy. As the W concentration increased to 9.4 at.%, a shoulder peak with a lower energy at about 283.5 eV appeared, and the peak intensity increased with W concentration. Generally, the peak at the range of 283.1–283.6 eV was assigned to the C—W bond [14–15]. Fig. 3d compiles the high-resolution XPS for the W 4f at the W concentration of 9.4 at.%. For metallic tungsten, the binding energy of W $4f_{7/2}$ peak was located at about 31.4–31.8 eV, while it

was located at about 32.2–32.4 eV for stoichiometric WC [16–18]. In this work the fitted position for W $4f_{7/2}$ peak was at 31.9 eV corresponding to the WC_{1-x} phase, which was consistent with the previous report [17,19]. It could be deduced that the tungsten carbide was formed due to the W addition and the chemical reaction between C and W atoms.

To make clear the intermediate carbon bonding state, Raman spectroscopy as a non-destructive tool was used to characterize the C—C structure [20]. The Raman analysis results are shown in Fig. 4. It presented the corresponding peak area ratio of D-peak to G-peak (I_D/I_G) and G peak position of the films as a function of the doped metal concentration. For Cu-DLC films, the I_D/I_G ratio (Fig. 4a) increased from 0.9 to 2.4 with Cu concentration, and the G peak position shifted from 1536 cm^{-1} to 1557.6 cm^{-1}. This revealed that the content and size of the sp^2-C phase organized in rings increased as the Cu concentration increased. For W-DLC films with low W concentration (<9.4 at.%), the I_D/I_G ratio increased and G peak position shifted towards high wave number, implying the increase of sp^2/sp^3 ratio with the W doping. But with the W concentration further increased to 12.6 at.%, the sp^2/sp^3 ratio decreased subsequently according to the decrease of the I_D/I_G ratio and G peak position. The result in the W-DLC film with the concentration of 31.9 at.% was excluded because the broaden peak was not
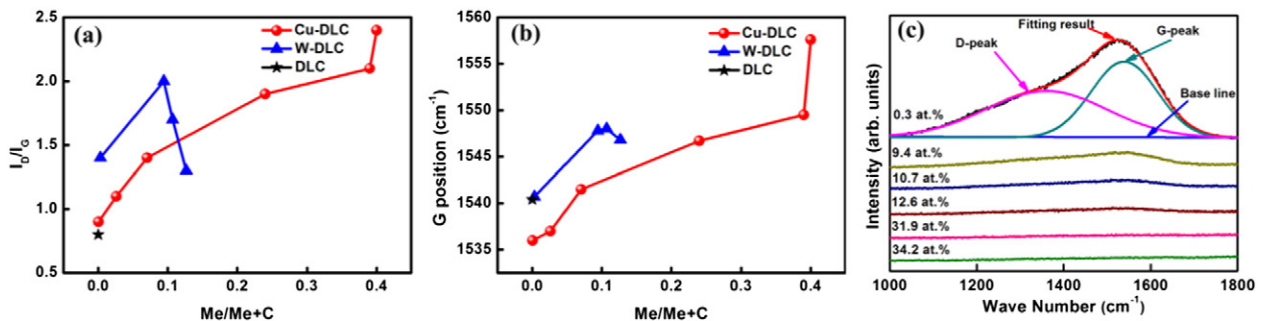

Fig. 4. (a) I_D/I_G for Cu-DLC and W-DLC films, (b) the G position of Cu-DLC and W-DLC films, (c) Raman spectra of W-DLC films.

observed in Fig. 4c, attributing to the increased W carbide which induced the decrease of C fraction in per unit area to the Raman scattering. The increase of sp^2/sp^3 ratio at the low W concentration might attribute to the decrease of local carbon atom density by binding carbon atoms into carbide, which could result in the graphitization [21]. However, with the W concentration increased, more sp^2-C participated in the formation of carbide nanocrystal because the bonding energy of sp^2-C was relatively lower than that of sp^3-C [22]. Consequently, as W concentration increased, more sp^2-C were used to form carbide phase and resulted in the decrease of sp^2-C fraction. Besides, the I_D/I_G ratio of W-DLC films was higher than that of the pure DLC, which was attributed to the introduction of W in the Me-DLC films acting as a catalyst to promote graphitization [23]. These results suggested that the graphitization in DLC films could be occurred with Cu or W addition.

Fig. 5 shows the plan-view TEM images and corresponding selected area electron diffraction (SAED) patterns of the Cu-DLC and W-DLC films. Both of the Cu-DLC film (Cu 7.0 at.%) and W-DLC film (W 9.4 at.%) presented a nanocomposite structure of amorphous carbon matrix compounded with metal or metal carbide nanocrystals. For Cu-DLC film, the SAED showed the existence of elemental copper and a polycrystalline pattern in the film, and the distinct rings displayed in the diffraction patterns were identified to be (111), (200), (220) and (311) reflections of the face-centered (FCC) Cu crystal. The copper nanoparticles were 3–5 nm in size and highly dispersed in the amorphous carbon structure. Meanwhile, the carbon network structure was still maintained. For W-DLC film, the WC_{1-x} phases with different orientations were identified, and a large amount of carbide phases broke the continuity of carbon network, leading to a completely different structure compared with Cu-DLC film. These were in accordance with the previous XPS results as shown in Fig. 3.

3.4. Surface topography

The 3D and 2D topographies of pure DLC, Cu-DLC (Cu 7.0 at.%) and W-DLC (W 9.4 at.%) are displayed in Fig. 6. The pure DLC film showed a smooth and flat surface with the roughness around 0.518 nm. The roughness values of Cu-DLC and W-DLC were 3.28 and 0.943 nm, respectively. For the Cu-DLC film, the nanostructure of elongated domes shape was observed in Fig. 6b, and the Cu nanosphere particulates dispersed in the film observed from Fig. 6e. Besides, it was proved that

the surface roughness of Cu-DLC films increased with the Cu concentration in our previous work [24]. Unlike Cu-DLC, there was no apparent tungsten carbide nanocrystal shown in W-DLC film (Fig. 6f), which might be attributed to the reaction between W and C atoms. But the size of the WC_{1-x} crystal also increased with the W concentration [25].

3.5. Analysis of the wetting mechanism

In order to obtain insight into the wetting mechanism of W-DLC and Cu-DLC films, the SE of films and their corresponding polar and dispersive components were quantified by applying the Owens-Wendt-Rath-Kaeble (OWRK) method [26]. Most methods for SE determination begin with the Young equation [27], which can be expressed as

$$\gamma_l \cos\theta = \gamma_s - \gamma_{sl} \tag{1}$$

where θ is the measured contact angle; γ_l, γ_s, and γ_{sl} are the surface energy of liquid, solid, and the liquid-solid interface, respectively. The equation describes the energy balance of a liquid (such as water) drop on solid surface.

In general, the SE can be divided into two components, dispersive component γ^d and polar component γ^p. The equations are as following

$$\gamma_l = \gamma_l^d + \gamma_l^p \tag{2a}$$

and

$$\gamma_s = \gamma_s^d + \gamma_s^p \tag{2b}$$

where γ_l^d and γ_l^p are the dispersive and polar components of surface free energy of the measured liquid, respectively; and γ_s^d and γ_s^p are the dispersive and polar components of SE of the solid, respectively.

According to the OWRK, the interfacial free energy γ_{sl} can be given in terms of the free energies of the liquid and solid phases; that is,

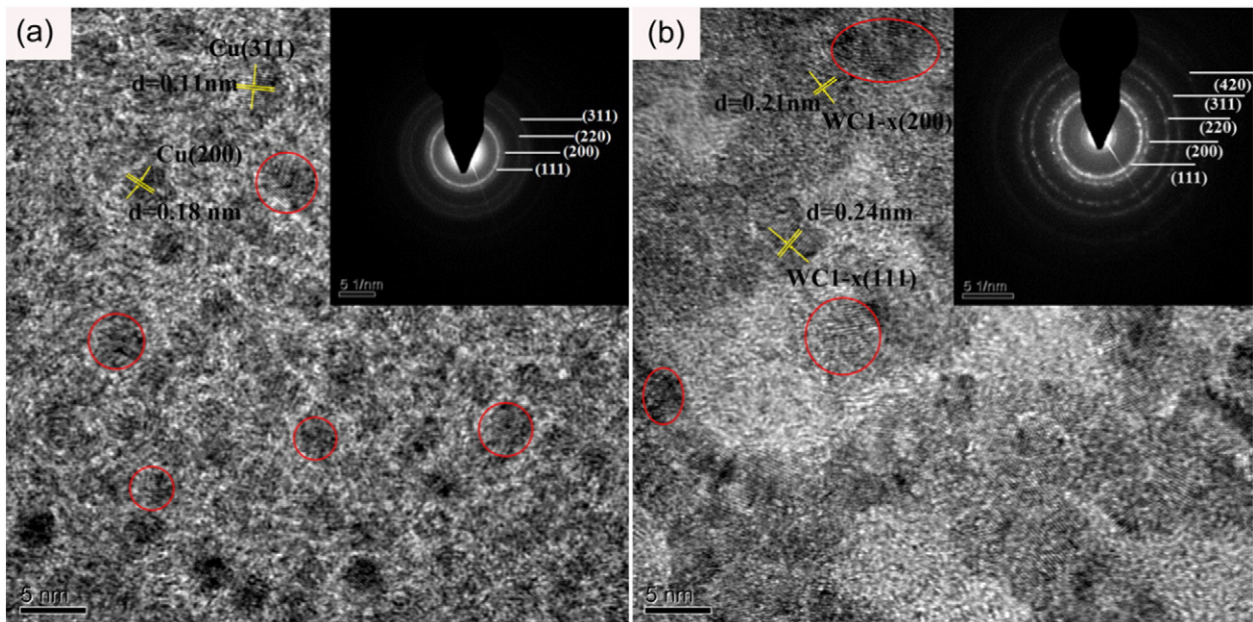$$\gamma_{sl} = \gamma_s + \gamma_l - 2\sqrt{\gamma_s^d \gamma_l^d} - 2\sqrt{\gamma_s^p \gamma_l^p} \tag{3}$$

Fig. 5. Typical HRTEM images and corresponding SAED patterns of Me-DLC films: (a) 7.0 at.% Cu-DLC, (b) 9.4 at.% W-DLC.
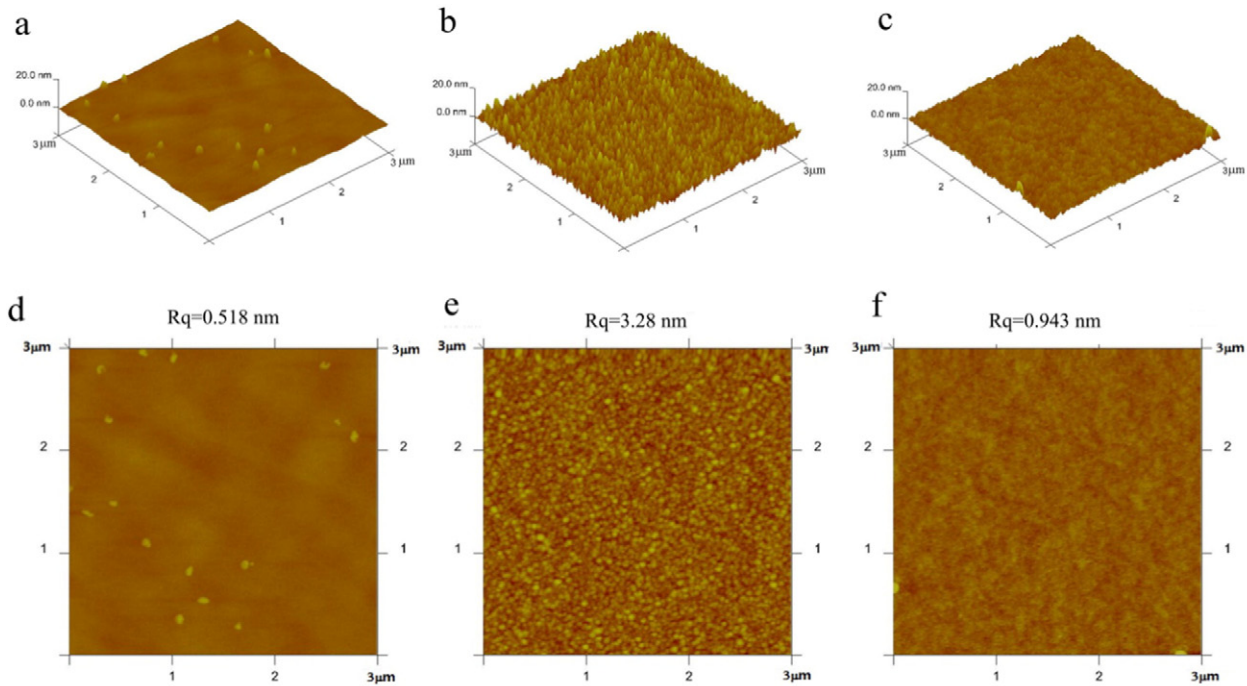
Fig. 6. Topographical AFM 3D and 2D images of pure DLC and Me-DLC: (a) (d) pure DLC, (b) (e) 7.0 at.% Cu-DLC, (c) (f) 9.4 at.% W-DLC.

The combination of both OWRK and Young equations gives:

$$1 + \cos\theta = 2\sqrt{\gamma_s^d}\left(\frac{\sqrt{\gamma_l^d}}{\gamma_l}\right) + 2\sqrt{\gamma_s^p}\left(\frac{\sqrt{\gamma_l^p}}{\gamma_l}\right) \qquad (4)$$

Using Eq. (4), a set of equations for two liquids with known polar and dispersive components (de-ionized water with $\gamma^p = 51.0$ mJ/m²; $\gamma^d = 21.8$ mJ/m² and diiodomethane with $\gamma^p = 0$ mJ/m²; $\gamma^d = 50.8$ mJ/m²) can be solved [28].

Results of SE and its components for W-DLC and Cu-DLC films are shown in Fig. 7. For Cu-DLC, it was obvious that SE of films significantly decreased when the content of Cu was >7.0 at.%. Remarkably, the decrease of SE was mainly due to the decrease of its polar component. The polar component of Cu-DLC (Cu < 7.0 at.%) was 6.19 ± 0.398 mN/m, but it decreased to 0.84 ± 0.421 mN/m when the Cu concentration was over 7.0 at.%. Unlike Cu-DLC, the SE of W-DLC films increased with W concentration, which was mainly due to the increase of its dispersive component, while the polar component kept around 5.37 ± 1.593 mN/m. Since the electric dipole of water molecule was attracted by the polar component of solid surface, it could be concluded that the polar component of SE played a major role in the different wetting properties between Cu-DLC and W-DLC films.

It is well known that the SE arises from the unbalance of the force between atoms or molecules inside and interfaces [7]. Generally, the polar component results from permanent and induced dipoles and hydrogen bonding. For Cu-DLC, the decrease of polar component could be attributed to the formation of graphitization and no formation of permanent dipole. Firstly, the sp²-rich surface could lower the polar component of SE. According to the related references [29–30], the values of surface energies for (100) and (111) planes of diamond calculated from the broken bond concept were 9207 and 3387 mJ/m², respectively, while that of basal plane of pyrolytic graphite was 1139 mJ/m². Thus, a sp²-rich surface could be responsible for the hydrophobic property by decreasing the dangling bonds. Secondly, there was no permanent dipole appeared owing to the existence of Cu elementary substance. Thus, the polar component of Cu-DLC film decreased with Cu addition, which was indicative of a decrease in reactivity of the film surface. In the case of W-DLC, the appearance of dipoles during the formation of W—C bonds could result in the increase of polar component. On the other hand, the increased sp²-C bond led to reduce the polar component [4,31]. Thus the two competitive factors maintained the value of the polar component.
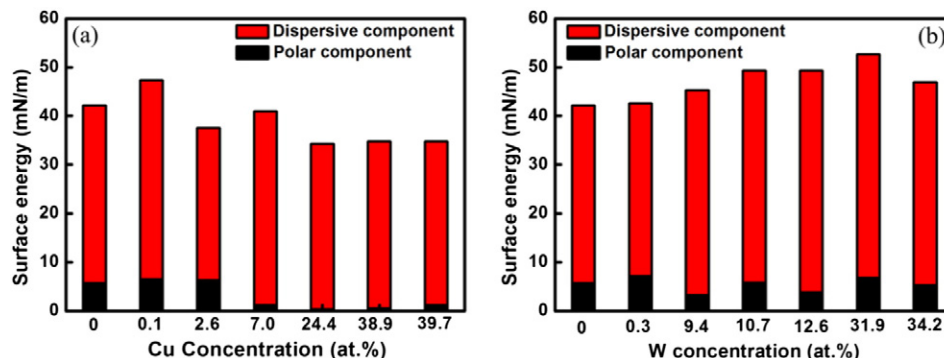

Fig. 7. The surface energy of the Me-DLC films with metal concentration: (a) Cu-DLC; (b) W-DLC.
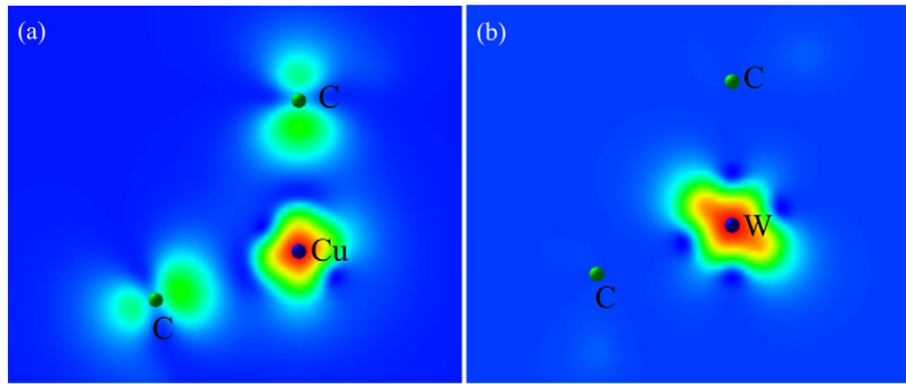
Fig. 8. The characteristics of HOMO of (a) Cu—C and (b) W—C systems.

In order to gain insight into the mechanism of the wettability on electronic scale, the first-principles calculations were performed to investigate the electronic structure of W—C and Cu—C systems using the tetrahedral cluster model, which are shown in Fig. 8. It was obvious that the characteristics of highest occupied molecular orbital (HOMO) was anti-bonding for Cu element incorporation (Fig. 8a). Li et al. [4] revealed that the anti-bonding characteristic between Cu and C atoms significantly weakened the bond strength and the stability of the system, and Chen et al. [32] also clarified that Cu bonded very weakly with carbon and formed no carbide phase. Therefore, the Cu metallic clusters could be easily formed in a carbon-based matrix with Cu concentration, causing the absence of permanent dipole moment [8]. For W-DLC films, the charge density of HOMO was isolated around the central W atom as illustrated in the Fig. 8b. It evidently revealed that the bond characteristic between W and C atoms was non-bonding, and the formed W—C bonds resulted in the appearance of dipoles which led to the hydrophilicity of W-DLC films.

Besides, the effect of surface roughness on the wettability of films is also very important. It is given by Wenzel's equation [33]:

$$\cos\theta_w = r\cos\theta_0 \tag{5}$$

where r is a roughness factor defined as the ratio of the actual and geometric area; θ_0 is a contact angle for an ideal smooth surface and θ_w is a contact angle for a rough surface. It was apparently shown that the roughness advantageously promoted the intrinsic wettability of materials, which meant a high roughness was beneficial to improve the hydrophobic property of hydrophobic materials, while it could decrease the WCA of hydrophilic materials. Thus, the Cu-DLC got more hydrophobic with Cu concentration, while the W-DLC kept in the hydrophilic range with W concentration. It meant that the roughness of both films played a positive role in promoting their intrinsic wetting properties. In view of the results described above, it could be concluded that increasing the size and quantity of Cu and W—C particles might further improve the intrinsic wettability of both Cu-DLC and W-DLC films.

4. Conclusion

Cu-DLC and W-DLC films were synthesized by a hybrid ion beam deposition system. The doped Cu and W concentrations in the films ranged from 0.1 to 39.7 at.% and from 0.3 to 34.2 at.%, respectively. The results revealed that the Cu and W doping showed different influences on the surface wetting of DLC films. For Cu-DLC films, the increase of Cu concentration caused the transformation from hydrophilic state to hydrophobic state, while the water contact angle of W-DLC kept in a hydrophilic range within the presented W concentration. The comprehensive results of surface energy and first-principles calculations revealed that, the anti-bonding characteristic formed between Cu and C atoms led to the absence of permanent dipoles and decreased the surface

energy of Cu-DLC films, causing the transformation from hydrophilic to hydrophobic behavior. However, the nonbonding characteristic was obtained between carbide-forming metal W and C atoms, which caused the presence of dipoles of W—C bonds, and thereafter resulted in the increase of surface energy of films. Moreover, different bonding characteristic also made a positive contribution to the sp^2/sp^3 ratio and surface roughness, which had a profound effect on the wettability of films. In summary, the different atomic bond characteristic between metal and C atoms could be the fundamental reason of the wettability of Me-DLC films. The results here offer a facile strategy to design DLC films with tailored wettability properties together with other superior mechanical and tribological behaviors for the promising applications, such as biomedical implants, marine frictional components. For example, such hydrophobic Cu-DLC films could be used for protective antifouling window layer in marine [34].

References

[1] J. Robertson, Diamond-like amorphous carbon, Mater. Sci. Eng. R 37 (4–6) (2002) 129–281.
[2] D. Caschera, P. Cossari, F. Federici, S. Kaciulis, A. Mezzi, G. Padeletti, D.M. Trucchi, Influence of PECVD parameters on the properties of diamond-like carbon films, Thin Solid Films 519 (2011) 4087–4091.
[3] X. Li, P. Ke, A. Wang, Ab initio molecular dynamics simulation on stress reduction mechanism of Ti-doped diamond-like carbon films, Thin Solid Films 584 (2015) 204–207.
[4] A.M. Asl, P. Kameli, M. Ranjbar, H. Salamati, M. Jannesari, Correlations between microstructure and hydrophobicity properties of pulsed laser deposited diamond-like carbon films, Superlattice. Microst. 81 (2015) 64–79.
[5] Y. Ma, X. Cao, X. Feng, Y. Ma, H. Zou, Fabrication of super-hydrophobic film from PMMA with intrinsic water contact angle below 90°, Polymer 48 (26) (2007) 7455–7460.
[6] L. Zhang, G. Lin, G. Ma, K. Wei, Z. Duan, Hydrophobic property of hydrogen-free Ti-DLC films, Rare Metal Mater. Eng. 42 (10) (2013) 2123–2126.
[7] J. Chen, S. Lau, Z. Sun, G. Chen, Y. Li, B. Tay, et al., Metal-containing amorphous carbon films for hydrophobic application, Thin Solid Films 398–399 (2001) 110–115.
[8] L. Ostrovskaya, V. Perevertailo, L. Matveeva, P. Milani, V. Ralchenko, E. Shpilevsky, Characterization of different carbon nanomaterials promising for biomedical and sensor applications by the wetting method, Powder Metall. Met. Ceram. 42 (1–2) (2003) 1–8.
[9] X. Li, K. Lee, A. Wang, Chemical bond structure of metal-incorporated carbon system, J. Comput. Theor. Nanosci. 10 (2013) 1688–1692.

[10] W. Dai, H. Zheng, G. Wu, A. Wang, Effect of bias voltage on growth property of Cr-DLC film prepared by linear ion beam deposition technique, Vacuum 85 (2) (2010) 231–235.

[11] A. Mezzi, S. Kaciulis, Surface investigation of carbon films: from diamond to graphite, Surf. Interface Anal. 42 (2010) 1082–1084.

[12] T. Ghodselahi, M.A. Vesaghi, A. Shafiekhani, A. Baghizadeh, M. Lameii, XPS study of the Cu@Cu$_2$O core-shell nanoparticles, Appl. Surf. Sci. 255 (2008) 2730–2734.

[13] L. Sun, P. Guo, P. Ke, X. Li, A. Wang, Synergistic effect of Cu/Cr co-doping on the wettability and mechanical properties of diamond-like carbon films, Diam. Relat. Mater. 68 (2016) 1–9.

[14] T. Takeno, T. Komiyama, H. Miki, T. Takagi, T. Aoyama, XPS and TEM study of W-DLC/DLC double-layered film, Thin Solid Films 517 (17) (2010) 5010–5013.

[15] Z. Fu, C. Wang, W. Zhang, W. Wang, W. Yue, X. Yu, et al., Influence of W content on tribological performance of W-doped diamond-like carbon coatings under dry friction and polyalpha olefin lubrication conditions, Mater. Des. 51 (2013) 775–779.

[16] C. Moreno-Castilla, M. Alvarez-Merino, F. Carrasco-Marin, J. Fierro, Tungsten and tungsten carbide supported on activated carbon: surface structures and performance for ethylene hydrogenation, Langmuir 17 (2001) 1752–1756.

[17] A. Voevodin, J. O'Neill, S. Prasad, J. Zabinski, Nanocrystalline WC and WC/a-C composite coatings produced from intersected plasma fluxes at low deposition temperatures, J. Vac. Sci. Technol. A 17 (3) (1999) 986–992.

[18] J. Moulder, W. Stickle, P. Sobol, K. Bomben, Handbook of X-ray Photoelectron Spectroscopy, Physical Electronics, Eden Prairie, 1995 216–241.

[19] Y. Pauleau, P. Gouy-Pailler, Characterization of tungsten-carbon layers deposited on stainless steel by reactive magnetron sputtering, J. Mater. Res. 7 (8) (1992) 2070–2079.

[20] Y. Liu, L. Ojamäe, C—C stretching Raman spectra and stabilities of hydrocarbon molecules in natural gas hydrates: a quantum chemical study, J. Phys. Chem. A 118 (49) (2014) 11641–11651.

[21] A.A. Voevodin, M.A. Capano, S.J.P. Laube, M.S. Donley, J.S. Zabinski, Design of a Ti/TiC/DLC functionally gradient coating based on studies of structural transitions in Ti—C thin films, Thin Solid Films 298 (1–2) (1997) 107–115.

[22] W. Dai, P. Ke, M. Moon, K. Lee, A. Wang, Investigation of the microstructure, mechanical properties and tribological behaviors of Ti-containing diamond-like carbon films fabricated by a hybrid ion beam method, Thin Solid Films 520 (19) (2012) 6057–6063.

[23] K. Bewilogua, R. Wittorf, H. Thomsen, M. Weber, DLC based coatings prepared by reactive d.c. magnetron sputtering, Thin Solid Films 447–448 (2004) 142–147.

[24] P. Guo, L. Sun, X. Li, S. Xu, P. Ke, A. Wang, Structural evolution and surface wettability of Cu-containing diamond-like carbon films by a hybrid linear ion beam deposition technique, Thin Solid Films 584 (2015) 289–293.

[25] P. Guo, P. Ke, A. Wang, Incorporated W roles on microstructure and properties of W—C:H films by a hybrid linearion beam systems, J. Nanomater. 2013 (2013) s1–s8.

[26] D.K. Owens, R.C. Wendt, Estimation of the surface free energy of polymers, Appl. Polym. Sci. 13 (1969) 1741–1747.

[27] T. Young, An essay on the cohesion of fluids, Philos. Trans. R. Soc. Lond. 9 (1805) 65–87.

[28] D. Banerjee, S. Mukherjee, K. Chattopadhyay, Controlling the surface topology and hence the hydrophobicity of amorphous carbon thin films, Carbon 48 (4) (2010) 1025–1031.

[29] T. Takai, Reconstruction and energetics for surface of silicon, diamond and β-SiC, Surf. Sci. Lett. 164 (2) (1985) 341–352.

[30] S.K. Rhee, Critical surface energies of Al$_2$O$_3$ and graphite, J. Am. Ceram. Soc. 55 (6) (2006) 300–303.

[31] L. Ostrovskaya, Studies of diamond and diamond-like film surfaces using XAES, AFM and wetting, Vacuum 68 (3) (2002) 219–238.

[32] C. Chen, F. Hong, Structure and properties of diamond-like carbon nanocomposite films containing copper nanoparticles, Appl. Surf. Sci. 242 (2005) 261–269.

[33] A. Neumann, Contact angles and their temperature dependence: thermodynamic status, measurement, interpretation and application, Adv. Colloid Interf. Sci. 4 (2–3) (1974) 105–191.

[34] Y. Liu, P. Guo, X. He, L. Li, A. Wang, H. Li, Developing transparent copper-doped diamond-like carbon films for marine antifouling applications, Diam. Relat. Mater. 69 (2016) 144–151.